

## Jet Modification in Heavy Ion Collisions at RHIC

M. van Leeuwen

*Universiteit Utrecht, PO Box 80000, Utrecht, Netherlands*

These proceedings present a brief overview of the main results on jet-modifications in heavy ion collisions at RHIC. In heavy ion collisions, jets are studied using single hadron spectra and di-hadron correlations with a high- $p_T$  trigger hadrons. At high  $p_T$ , a suppression of the yields due to parton energy loss is observed. A quantitative confrontation of the data with various theoretical approaches to energy loss in a dense QCD medium is being pursued. First results from  $\gamma$ -jet events, where the photon balances the initial jet energy, are also presented and compared to expectations from models based on di-hadron measurements. At intermediate  $p_T$ , two striking modifications of the di-hadron correlation structure are found in heavy ion collisions: the presence of a long-range *ridge* structure in  $\Delta\eta$ , and a large broadening of the recoil jet. Both phenomena seem to indicate an interplay between hard and soft physics.

The goal of research with high-energy nuclear collisions at the Relativistic Heavy Ion Collider (RHIC) is to study bulk matter systems where the strong nuclear force as described by Quantum Chromo Dynamics (QCD) is the dominant interaction. In particular, it is expected that there is a phase transition of bulk QCD matter to a deconfined state at high temperature. In heavy ion collisions, like in other hadronic collision, most produced particles are hadrons with low momenta. Experimental results at RHIC have shown collective behaviour in the in the soft sector, such as elliptic flow, which is a strong indication that indeed 'bulk QCD matter' is created in collisions at RHIC [1, 2, 3, 4].

Products of initial state hard scatterings, such as high- $p_T$  hadrons, photons and heavy mesons, can be used to probe the soft matter. Initial state production of high- $p_T$  partons is relatively unaffected by the presence of the soft medium, but the partons lose energy when traversing the medium, dominantly due to gluon radiation. The goal of high- $p_T$  measurements is to study these interactions and to use them to measure the density and temperature of the soft matter.

### I. MEDIUM DENSITY FROM HADRON SPECTRA AND DI-HADRONS

The first indications of parton energy loss in the hot and dense matter come from inclusive spectra measurement. To quantify the suppression of particle production in heavy ion collisions, the nuclear suppression factor

$$R_{AA}(p_T) = \frac{dN/p_T dp_T dy|_{Au+Au}}{N_{bin} dN/p_T dp_T dy|_{p+p}}, \quad (1)$$

i.e. the ratio of the measured spectrum  $dN/p_T dp_T dy$  in Au+Au and p+p collisions, is used. The factor  $N_{bin}$  is the number of underlying binary nucleon-nucleon collisions in the heavy ion collisions which is calculated using a geometrical model of the collision [5].

Figure 1 shows  $R_{AA}$  as measured in central Au+Au collisions at RHIC. For direct photons (solid squares)  $R_{AA} \approx 1$ , indicating that the cross section for hard production processes scales with  $N_{bin}$  for particles that do not interact strongly with the medium. For light hadrons,  $\pi^0$  and  $\eta$ , on the other hand, a suppression by a factor 4–5 ( $R_{AA} \approx 0.2$ ) is seen, signaling strong interactions of the partons with the medium.

The jet-structure of high- $p_T$  hadron production in heavy ion collisions is explored using azimuthal di-hadron correlation measurements. Figure 2 shows distributions of the angle between a trigger hadron at high  $p_T^{trig}$  and associated hadrons at lower  $p_T^{assoc}$ . For the higher  $p_T^{trig}$  selections, there are two clear correlation peaks due to the near-side ( $\Delta\phi \approx 0$ ) and the recoil ( $\Delta\phi \approx \pi$ ) jet. The peaks sit on top of a combinatorial background, which is subtracted to obtain associated yields.

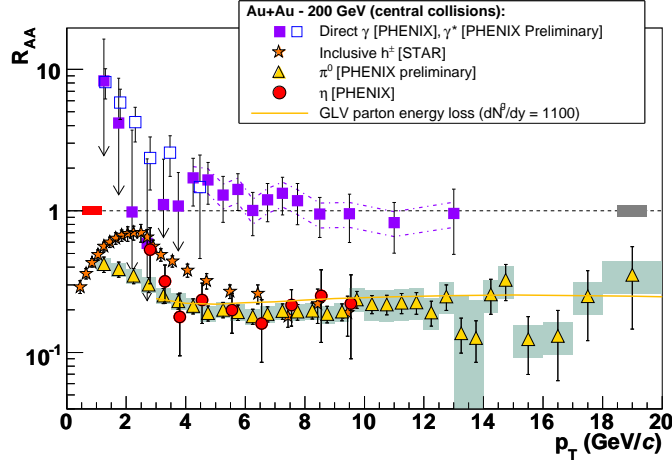


FIG. 1: Nuclear suppression ratio  $R_{AA}$  (see text) as a function of  $p_T$  for  $\gamma$ ,  $\pi^0$  and  $\eta$  in central Au+Au collisions at  $\sqrt{s_{NN}}=200$  GeV [6].

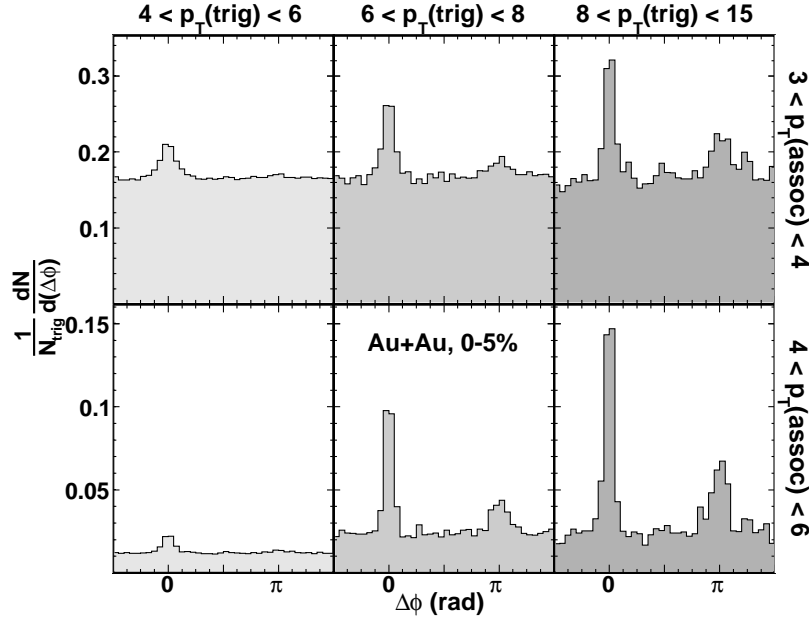


FIG. 2: Per-trigger normalised azimuthal distribution of charged particles associated with high- $p_T$  trigger particles in central Au+Au collisions for different  $p_T$ -selections for the trigger ( $p_T^{trig}$ ) and associated particles ( $p_T^{assoc}$ ) [7].

Figure 3 shows the near-side (left panel) and recoil yield (right panel) associated per-trigger yields for trigger hadrons with  $8 < p_T^{trig} < 15$  GeV/c, for d+Au collisions and Au+Au collisions with two different centralities, 20-40% and 0-5% of the total hadronic cross section. It can clearly be seen that the near side yield is similar in d+Au and Au+Au collisions, while the recoil yield shows a suppression which increases with centrality. The per-trigger normalisation of the yield compensates for the overall scaling of the number of hard scatterings, due to the larger volume in Au+Au collisions ( $N_{bin}$  scaling in  $R_{AA}$ ), as well as the leading hadron suppression. The associated hadron yield on the near-side measures the secondary fragment distribution given a high- $p_T$  trigger particle. The fact that this distribution does not change from d+Au to Au+Au collisions, indicates that partons fragment in the same way in d+Au collisions as in Au+Au collisions after energy loss. The recoil yield, on the other hand, measures the distribution of (leading) hadrons in the jet opposite to the trigger hadron and the suppression of this yield is a

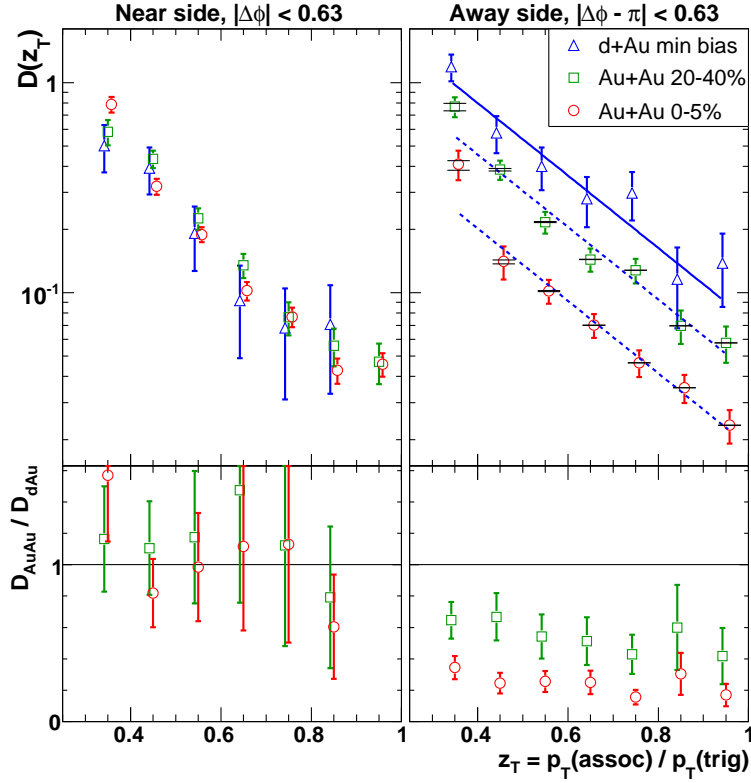


FIG. 3: Near-side (left panel) and recoil (right panel) associated per-trigger yields for trigger hadrons with  $8 < p_T^{trig} < 15$  GeV/c, for d+Au collisions and Au+Au collisions at two different centralities, 20-40% and 0-5% of the total hadronic cross section [7]. The lower panels shows ratios of the Au+Au results to the d+Au reference.

measure of parton energy loss.

### A. Quantitative analysis of medium density

QCD gluon radiation off high-energy partons in a dense QCD medium is modeled using a number of different approximations. There are four main calculational frameworks of which two are based on the BDMPS-Z path integral formalism for multiple scattering in a static medium, including Landau-Pomeranchuk-Migdal interference effects [8, 9]. Two approximations exist in this framework: the multiple-soft-scattering approach, as originally proposed by BDMPS and further worked out for modeling applications by Salgado and Wiedemann [10], and the few-hard-scattering approach that was proposed originally by Gyulassy, Levai and Vitev (GLV) [11]. The two other approaches are based on a higher-twist formalism, inspired by Deeply Inelastic Scattering [12] and the Hard Thermal Loop high-temperature QCD formalism (AMY [13]). It is important to realise that there are still a number of open theoretical questions, such as the effect of collisional energy loss (non-static medium)[14, 15] and finite-energy effects.

Now that the experimental data have a large  $p_T$ -reach (up to 18 GeV/c for the  $\pi^0$  spectra) and reasonably small statistical+systematic uncertainties, various groups are exploring systematic confrontations of theories with the data [16, 18]. A recent advance is the quantitative treatment of systematic uncertainties on the measurements [19] in these comparisons.

Figure 4 the expected nuclear modification factor  $R_{AA}$  for several different medium densities from one energy loss model [16] compared to the measured values. The right panel shows the modified  $\chi^2$  (which accounts for systematic effects, see [19]) as a function of the medium density which is quoted as the mean transport coefficient  $\langle \hat{q} \rangle$ . The transport coefficient  $\hat{q}$  is the squared momentum transfer per unit path length which characterises the energy loss

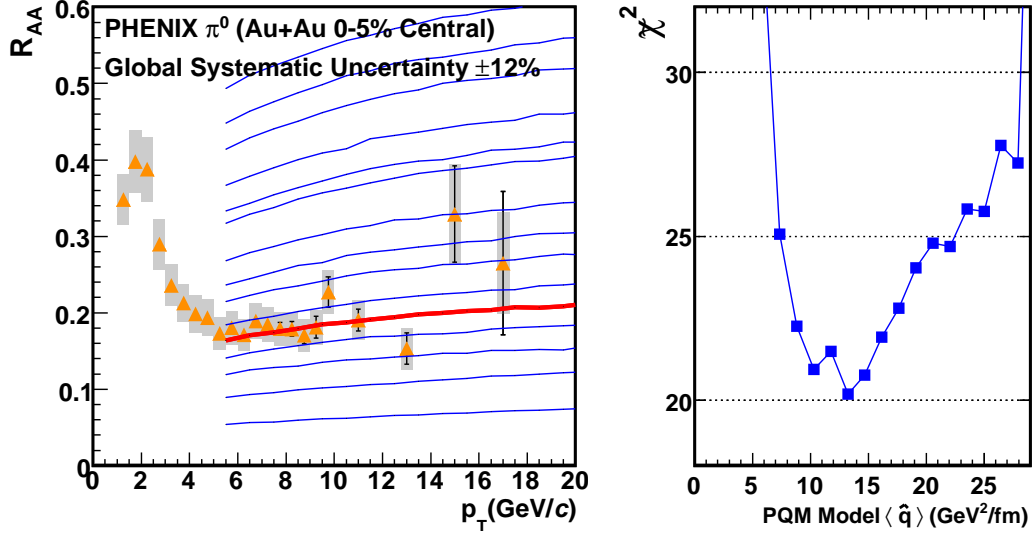


FIG. 4: Measured nuclear modification factor  $R_{AA}$  for  $\pi^0$ , compared to model calculations [16] based on the BDMPs formalism. The right panel shows the modified  $\chi^2$  of data compared to the model curves, including systematic uncertainties [17].

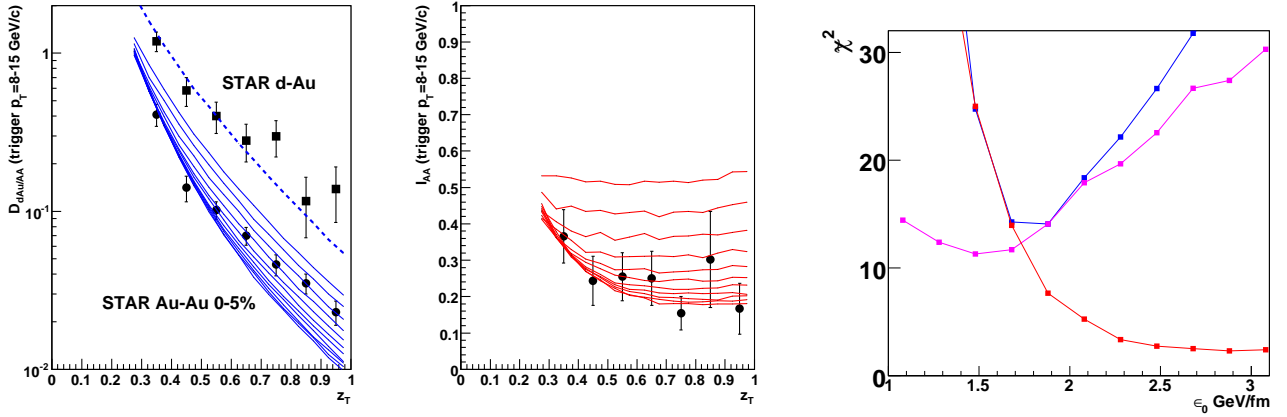


FIG. 5: Measured suppression of the recoil yield with trigger particles  $8 < p_T^{trig} < 15$  GeV/c compared to model calculations [18]. The left panel shows the recoil yield  $D_{AA}$  for d+Au and Au+Au collisions, the middle panel the suppression ratio  $I_{AA}$  and the right panel shows the modified  $\chi^2$  of data compared to the model curves, including systematic uncertainties. Three different  $\chi^2$  values are given, using the recoil spectrum  $D_{AA}$  (blue line), including theory uncertainty on the reference (magenta line) and using the measured ratio Au+Au suppression  $I_{AA}$  (red curve) [20].

properties of the medium. The mean energy loss  $\Delta E \propto \alpha_s \hat{q} L^2$  for a static medium [10]. The extracted value of the mean transport coefficient  $\langle \hat{q} \rangle = 13.2^{+2.1}_{-3.2}$  GeV<sup>2</sup>/fm, based on this model. A number of other models have also been compared to the data [19, 20] and tend to give lower estimates of the (equivalent) medium density.

Figure 5 (left panel) shows the recoil yield for trigger particles with  $8 < p_T^{trig} < 15$  GeV/c in d+Au and Au+Au collisions compared to model curves with different medium density. The right panel shows again the modified  $\chi^2$  as a function of density. The model used in this case is a higher twist model, because the full set of calculations for the recoil yield has so far only been performed for that model [18]. The model parameter in this case is the typical energy loss  $\epsilon_0$ . Because the d+Au reference measurement for this observable has only limited statistical precision, a few different approaches were taken for the theory fit. Firstly, one can directly fit the recoil yield, assuming that

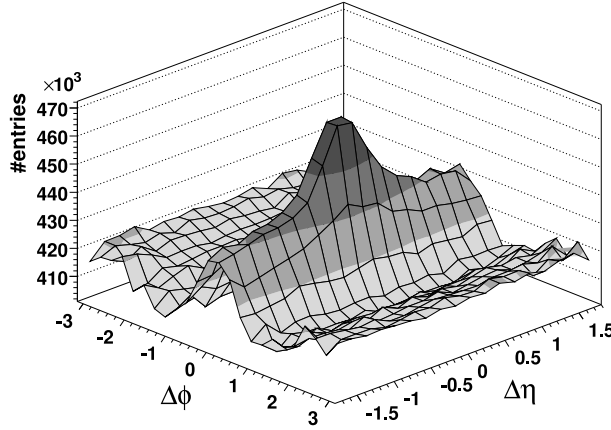


FIG. 6: Distribution of associated hadrons with  $2 < p_T^{assoc} < 3$  GeV/c in pseudo-rapidity  $\eta$  and azimuthal angle  $\phi$  with respect to a trigger particle with  $3 < p_T^{trig} < 4$  GeV/c in central Au+Au collisions at RHIC [21].

the NLO calculation correctly describes the p+p result. The resulting  $\chi^2$  is shown by the blue curve in Fig. 5. The best-fit value for  $\epsilon_0 \approx 1.9$  is compatible with the value extracted using the single-hadron data with this same model  $\epsilon_0 = 1.9^{+0.2}_{-0.5}$  GeV/fm [20]. Adding the scale uncertainty on the calculated d+Au reference yield gives the magenta curve. When the d+Au measurement is used to calculate the recoil suppression  $I_{AA}$ , the red curve is obtained. This last procedure is the most similar to what was done for the single particle suppression in Fig. 4, but it gives the weakest constraint on  $\epsilon_0$ . Future high-statistics measurements of di-hadron correlations in p+p and d+Au collisions at RHIC will further constrain the theory in this area.

## II. INTERMEDIATE $p_T$ : RIDGE AND DOUBLE-HUMP

Di-hadron correlation measurements at lower  $p_T$  show large qualitative differences between p+p reference measurements and Au+Au results. Two specific striking features are widely discussed. One effect is the observation that there is significant associated yield at larger pseudo-rapidity difference  $\Delta\eta \gtrsim 0.7$ , which is not expected from jet fragmentation. The other observation is a large broadening of the recoil distribution at low  $p_T$ , to the point where the distribution becomes doubly-peaked.

Figure 6 shows the distribution of associated hadrons with  $2 < p_T^{assoc} < 3$  GeV/c in pseudo-rapidity  $\eta$  and azimuthal angle  $\phi$  with respect to a trigger particle with  $3 < p_T^{trig} < 4$  GeV/c in central Au+Au collisions at RHIC [21]. At these  $p_T$ , the associated hadrons show not only the jet-like peak around  $(\Delta\eta, \Delta\phi) = (0, 0)$ , but also significant additional associated yield at larger  $\Delta\eta$ . The additional yield is approximately uniformly in  $\Delta\eta$  and therefore it is referred to as *ridge*-yield. The *ridge*-effect is unique to heavy ion collisions and is found to be present for trigger hadrons over the entire accessible  $p_T$ -range (up to 7 GeV/c at present) [21]. The strength of the jet-like peak increases with  $p_T^{trig}$ , so that the relative contribution of the ridge to the near-side yield decreases with higher  $p_T^{trig}$ . A number of different possible production mechanisms have been proposed, such as coupling of radiated gluons to longitudinal flow [22, 23, 24], medium heating by the passage of a hard parton combined with longitudinal flow [25] and a radial flow boost to the underlying p+p event, combined with trigger bias [26, 27]. Further experimental work is going on to distinguish the different scenarios.

Another striking finding from di-hadron correlations at intermediate  $p_T$  is that the away-side peak is strongly broadened. This is illustrated in Figure 7, which shows associated hadron distributions with  $1 < p_T^{assoc} < 2.5$  GeV/c for three different ranges of  $p_T^{trig}$  in central Au+Au collisions [28] (full symbols). The open symbols in the Figure show d+Au results for reference. Clearly, the away-side distribution is strongly broadened in the Au+Au collisions, compared to d+Au collisions. For lower  $p_T^{trig}$ , there might even be a minimum in the distribution at  $\Delta\phi = \pi$ . This observation has lead to the suggestion that partons propagating through the strongly interaction medium may give

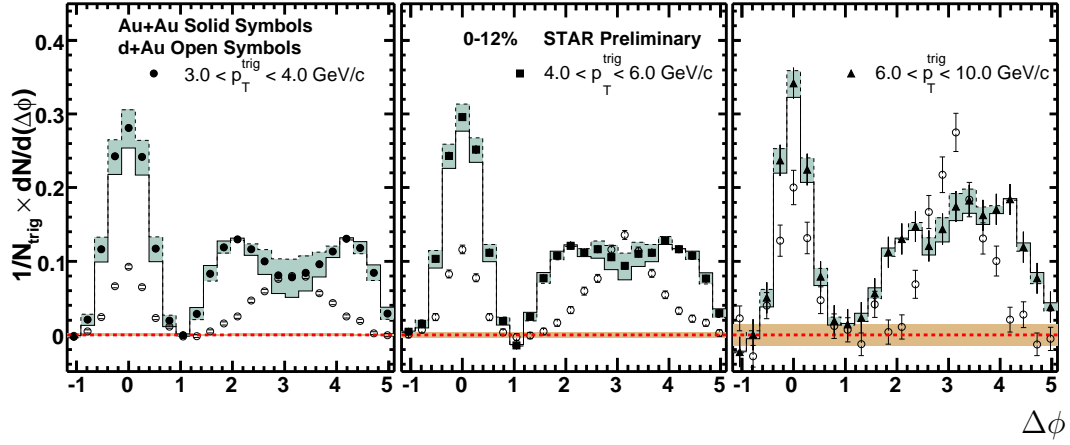


FIG. 7: Background-subtracted distribution of associated hadrons with  $1 < p_T^{assoc} < 2.5$  GeV/c for three different ranges of  $p_T^{trig}$ , in central Au+Au collisions at  $\sqrt{s_{NN}}=200$  GeV (full symbols) and d+Au collisions (open symbols)[28]. The lines indicate the uncertainty on the signal shape due to the uncertainty in the elliptic flow of the background. The shaded bands around 0 indicate the statistical uncertainty on the background level.

rise to Mach-Cone shock waves [29, 30]. The width of the away-side distribution would then measure the opening angle and thus the velocity of sound in the medium. However, it has also been pointed out that gluon radiation in combination with the kinematic constraint  $p_T^{trig} \approx p_T^{assoc}$  may give rise to a broadened away-side (or even ‘Mercedes-events’) as well [31]. It is also important to realise that the raw signal sits on a large background which is not constant, but has a  $1 + \cos(2\Delta\phi)$  distribution due to elliptic flow. The background has been subtracted in Fig. 7 and the uncertainty on the extracted signal from the uncertainty in the strength of elliptic flow is indicated by the shaded band. However, possible correlations between elliptic flow and the jet-structure are not taken into account in this estimate.

Three-particle correlation measurements are currently being developed to further explore the away-side shapes.

### III. NEW RESULTS ON ENERGY LOSS AND OUTLOOK: $\gamma$ -JET AND JET RECONSTRUCTION

While the single hadron and di-hadron suppression in Au+Au collisions can be used to determine the average medium density, more detailed studies have shown that the both observables, but in particular the single hadron distribution, are relatively insensitive to details of the energy loss process, such as the probability distribution of energy loss [32]. This is because the initial jet energy is not constrained in the single-hadron measurement and only poorly constrained in the di-hadron measurement. In addition, the typical energy loss (for partons that lose energy; there is also a finite probability that no radiation occurs) can be as large as 10 GeV [33], which is large compared to the jet-energies at RHIC.

Currently, two types of measurement are being discussed that provide access to the initial jet energy before energy loss. The first method is to use  $\gamma$ -jet events, where the transverse momentum of the photon is equal to the initial jet-energy. The drawback of this method is the small cross section compared to hadron production, which translates in a limited kinematic reach. An alternative way to measure the initial parton energy is to perform full jet reconstruction. This method has potentially large statistics, but suffers from a large combinatorial background and is therefore mainly discussed for LHC [34, 35], although work is going on to perform jet-reconstruction in heavy ion events at RHIC as well.

Figure 8 shows first results from  $\gamma$ -jet pair in heavy ion collisions, which were presented by the STAR experiment at the recent Quark Matter conference in Jaipur [36] (see also [37] for a similar analysis from the PHENIX experiment). The Figure shows the centrality dependence of the suppression of the recoil yield ( $I_{AA}$ ) opposite  $\pi^0$  (left panel) and direct photons (right panel). The recoil suppression is found to be similar for  $\pi^0$  triggers and direct-photon

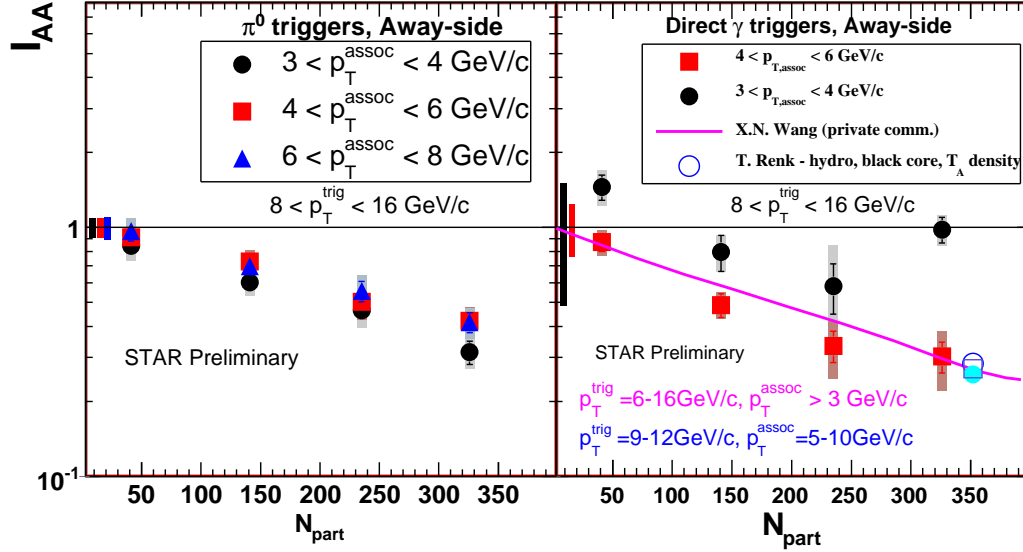


FIG. 8: Centrality dependence of the suppression of the recoil yield for leading  $\pi^0$  (left panel) and direct photons (right panel) with  $8 < E_\gamma < 10$  GeV [36].

triggers, and in agreement with theoretical predictions which are based on the di-hadron measurements presented in Figure 2. In the near future, differential measurements of the suppression as a function of hadron  $p_T$  will allow to experimentally constrain the probability distribution for parton energy loss in the medium [38].

In summary, high- $p_T$  jet production in heavy ion collisions has been observed at RHIC. The most direct signatures of jet and di-jet production are provided by di-hadron measurements and more recently in direct photon-jet events. At high  $p_T$  a clear suppression of the recoil jet is observed, indicating that the partons lose energy while propagating through the dense QCD matter formed in the collision. Systematic comparisons of single hadron spectra, di-hadron and  $\gamma$ -jet measurements to theory calculations are being pursued to obtain limits on the parton-medium interaction and on the medium properties themselves. Measurements with reconstructed jets and more detailed analysis of  $\gamma$ -jet events, which are expected in the next few years, are crucial to constrain energy loss models, because they provide a direct measure of the initial jet energy.

- 
- [1] J. Adams et al. (STAR), Nucl. Phys. **A757**, 102 (2005), [nucl-ex/0501009](#)
  - [2] K. Adcox et al. (PHENIX), Nucl. Phys. **A757**, 184 (2005), [nucl-ex/0410003](#)
  - [3] I. Arsene et al. (BRAHMS), Nucl. Phys. **A757**, 1 (2005), [nucl-ex/0410020](#)
  - [4] B.B. Back et al., Nucl. Phys. **A757**, 28 (2005), [nucl-ex/0410022](#)
  - [5] M.L. Miller, K. Reygers, S.J. Sanders, P. Steinberg, Ann. Rev. Nucl. Part. Sci. **57**, 205 (2007), [nucl-ex/0701025](#)
  - [6] D.G. d'Enterria, J. Phys. **G34**, S53 (2007), [nucl-ex/0611012](#)
  - [7] J. Adams et al. (STAR), Phys. Rev. Lett. **97**, 162301 (2006), [nucl-ex/0604018](#)
  - [8] R. Baier, Y.L. Dokshitzer, A.H. Mueller, S. Peigne, D. Schiff, Nucl. Phys. **B483**, 291 (1997), [hep-ph/9607355](#)
  - [9] B.G. Zakharov, JETP Lett. **63**, 952 (1996), [hep-ph/9607440](#)
  - [10] C.A. Salgado, U.A. Wiedemann, Phys. Rev. **D68**, 014008 (2003), [hep-ph/0302184](#)
  - [11] M. Gyulassy, P. Levai, I. Vitev, Nucl. Phys. **B571**, 197 (2000), [hep-ph/9907461](#)
  - [12] X.N. Wang, X.f. Guo, Nucl. Phys. **A696**, 788 (2001), [hep-ph/0102230](#)
  - [13] P. Arnold, G.D. Moore, L.G. Yaffe, JHEP **11**, 001 (2000), [hep-ph/0010177](#)
  - [14] S. Wicks, W. Horowitz, M. Djordjevic, M. Gyulassy, Nucl. Phys. **A784**, 426 (2007), [nucl-th/0512076](#)

- [15] M. Djordjevic, U. Heinz, Phys. Rev. **C77**, 024905 (2008), 0705.3439
- [16] A. Dainese, C. Loizides, G. Paic, Eur. Phys. J. **C38**, 461 (2005), hep-ph/0406201
- [17] A. Adare et al. (PHENIX) (2008), arXiv:0801.4020
- [18] H. Zhang, J.F. Owens, E. Wang, X.N. Wang, Phys. Rev. Lett. **98**, 212301 (2007), nucl-th/0701045
- [19] A. Adare et al. (PHENIX), Phys. Rev. **C77**, 064907 (2008), arXiv:0801.1665
- [20] J.L. Nagle (2008), 0805.0299
- [21] J. Putschke, J. Phys. **G34**, S679 (2007), nucl-ex/0701074
- [22] N. Armesto, C.A. Salgado, U.A. Wiedemann, Phys. Rev. Lett. **93**, 242301 (2004), hep-ph/0405301
- [23] A. Majumder, B. Muller, S.A. Bass, Phys. Rev. Lett. **99**, 042301 (2007), hep-ph/0611135
- [24] P. Romatschke, Phys. Rev. **C75**, 014901 (2007), hep-ph/0607327
- [25] C.B. Chiu, R.C. Hwa, Phys. Rev. **C72**, 034903 (2005), nucl-th/0505014
- [26] S.A. Voloshin, Nucl. Phys. **A749**, 287 (2005), nucl-th/0410024
- [27] C.A. Pruneau, S. Gavin, S.A. Voloshin, Nucl. Phys. **A802**, 107 (2008), arXiv:0711.1991
- [28] M.J. Horner (STAR), J. Phys. **G34**, S995 (2007), nucl-ex/0701069
- [29] H. Stoecker, Nucl. Phys. **A750**, 121 (2005), nucl-th/0406018
- [30] J. Casalderrey-Solana, E.V. Shuryak, D. Teaney, J. Phys. Conf. Ser. **27**, 22 (2005), hep-ph/0411315
- [31] A.D. Polosa, C.A. Salgado, Phys. Rev. **C75**, 041901 (2007), hep-ph/0607295
- [32] T. Renk, Phys. Rev. **C77**, 017901 (2008), arXiv:0711.1030
- [33] T. Renk, K. Eskola, Phys. Rev. **C75**, 054910 (2007), hep-ph/0610059
- [34] S.L. Blyth et al., J. Phys. **G34**, 271 (2007), nucl-ex/0609023
- [35] G. Baur et al., Eur. Phys. J. **32S2**, 69 (2004)
- [36] A.M. Hamed (STAR) (2008), arXiv:0806.2190
- [37] M. Nguyen (PHENIX) (2008), arXiv:0805.1225
- [38] T. Renk, Phys. Rev. **C74**, 034906 (2006), hep-ph/0607166